

# Off-design analysis of a TES-based electricity storage system

**Alberto Benato<sup>a</sup>, Matteo Pecchini<sup>b</sup>, Francesca De Vanna<sup>c</sup> and Anna Stoppato<sup>d</sup>**

<sup>a</sup> Department of Industrial Engineering, University of Padova, Padova, Italy, [alberto.benato@unipd.it](mailto:alberto.benato@unipd.it), CA

<sup>b</sup> Department of Industrial Engineering, University of Padova, Padova, Italy, [matteo.pecchini@phd.unipd.it](mailto:matteo.pecchini@phd.unipd.it)

<sup>c</sup> Department of Industrial Engineering, University of Padova, Padova, Italy, [francesco.devanna@unipd.it](mailto:francesco.devanna@unipd.it)

<sup>d</sup> Department of Industrial Engineering, University of Padova, Padova, Italy, [anna.stoppato@unipd.it](mailto:anna.stoppato@unipd.it)

## Abstract:

Carnot battery is considered one of the most promising technologies for large-scale electricity storage. Among the available configurations, the so-called Integrated Energy Storage System (I-ESS) developed by the University of Padova research group allows the use of components of unused gas turbine power generation units for storage purposes. In particular, during low-demand hours, the electricity generated in surplus by, e.g., wind and solar, is used in an electric heater to heat up the air sucked by a fan. When air passes through the tank composed of a packed bed of solid material, it heats the bed itself. Therefore, excess electricity is stored as sensible heat in the storage material. Air then leaves the tank and is released into the atmosphere. During peak demand hours, the heat stored in the packed bed is extracted and converted again into electricity using a modified gas turbine in which the combustion chamber is bypassed and replaced by the storage tank. Having established that the I-ESS configuration can compete with the other large-scale storage technologies, the focus of this work is on the I-ESS off-design performance during the discharge phase. An investigation that still lacks in the literature. To predict the behaviour of the plant in part-load, the characteristic curves of the turbine and the compressor are implemented into the mathematical model of the I-ESS. In this way, the influence of key parameters such as pressure ratio, turbine inlet temperature, and generated power is analysed for the different state of discharge of the tank. The parameter that most affects the discharge time is the temperature of the tank. In fact, for a temperature of 1200 K, the total discharge time is up to 35 h. The discharge efficiency reaches 25.3%.

## Keywords:

Renewable Energy, Thermal Energy Storage, Off-design, Part-load analysis, Carnot battery.

## 1. Introduction

Reducing CO<sub>2</sub> emissions from human activities is one of the most urgent challenges in our society, and the electricity sector is one of the most impactful in terms of greenhouse gas emissions. For this reason, the production of power from renewable energy sources (RES) is of crucial importance to boost the sector decarbonisation. However, variability and unpredictability, the distinctive traits of renewables such as wind and solar, are pushing the need to develop and install energy storage units (ES) to avoid mismatch between electricity supply and demand. Various ES technologies have been developed over the years, each with its features in terms of power, capacity, response time, etc. Due to these differences, ES technologies can be classified according to their role in grid regulation, the way adopted to store the electricity, the amount of storable energy, etc.

Among large-scale technologies, electrochemical (flow batteries, FBs) and mechanical storage (pumped hydro storage (PHS) and compressed air energy storage (CAES)) are considered mature and commercially available solutions. However, FBs suffer from a short lifespan, whereas PHS and CAES are subjected to stringent geographical constraints. In addition, CAES needs a fossil fuel stream, whereas PHS requires an almost constant water flow rate. Furthermore, the vast exploitation of suitable PHS installation sites (especially in Europe and the United States), coupled with the drawbacks mentioned above, limits the further spread of this mature technology.

In fact, in recent years, due to the need for new types of grid-scale ES, researchers have begun to look at *thermomechanical* storage. Among these technologies, there are liquid air energy storage (LAES) systems and the so-called *Carnot batteries* (CBs). The latter is one of the most promising solutions in the field of large-scale electricity storage, as underlined by both Vecchi et al. [1] and Lampasi et al. [2]. The general working principle of a CB is as follows: during the charge, electricity is converted into heat and stored as thermal energy. When power is requested from the grid, thermal energy is converted back into electricity and delivered to the grid.

Several types of CB have been studied over the years (i) using sensible and latent thermal energy storage (TES), (ii) performing the charge by direct electric heating, heat pumps and low-temperature waste heat, and (iii) discharging the system by means of different thermodynamic cycles such as the Rankine, Brayton-Joule, and Kalina cycles [3]. Despite the proposals, the most studied CB plant arrangement is the one named Pumped Thermal Energy Storage (PTES).

PTES is characterised by a high energy density, low self-discharge rate, no geographical limitations, and a small installation footprint. It is based on a high temperature heat pump cycle, which converts the off-peak electricity into thermal energy and stores it inside two man-made thermally isolated tanks (usually called 'thermal energy storage' (TES)): one hot (storing temperature from 500°C to 1000°C) and one cold (storing temperature ranging from -150°C to -70°C). During high-demand hours, the system is discharged. In this phase, a thermal engine cycle is adopted to convert stored thermal energy into electricity. The working fluid is a gaseous medium, air, or argon, while electricity is stored as sensible heat using inexpensive and solid materials such as concrete, gravel, or other common minerals [4–6]. In addition, PTES allows the use of components from existing out-of-market fossil-based thermal power plants.

The latter is the motivation that led the authors of this work to develop the Integrated Energy Storage System (I-ESS): a storage unit that can be embedded in unused or currently being decommissioned fossil-based power plants, as well as at the same installation site for wind and solar plants [7, 8].

Briefly, the plant stores electricity as sensible heat in a high-temperature artificial tank consisting of a packed bed. The I-ESS plant is an open cycle that adopts air as a working fluid in both the charging and delivery modes. The charging scheme consists of a high-temperature tank, a fan, an electric heater, an electric motor, and a heat exchanger, while the delivery unit is made up of a compressor, a turbine, an electric motor/generator and the same high-temperature tank. In practise, the power train is a gas turbine in which the high-temperature tank replaces the combustion chamber.

Compared to PHS and CAES, I-ESS does not suffer from geographical constraints and does not require a stable water flow, such as PHS, or a natural gas stream such as CAES. Unlike FBs, the I-ESS plant is characterised by a longer cycle life, whereas, compared to PTES, the I-ESS layout features a lower complexity. Despite the previously conducted studies demonstrated the feasibility of the I-ESS plant (see, e.g., [7, 8]), and its ability to be coupled with a variable renewable-based facility to smooth its variable production (see, e.g., [9]), it is necessary to investigate the off-design behaviour of the system during the discharge phase. This is a critical phase due to the need for fast matching the grid requirements; a fact that forces the I-ESS plant to operate in off-design conditions.

To this end, the mathematical model of the I-ESS is improved by implementing the performance maps of the turbomachines and a tailor-made control strategy in order to make the mathematical model able to predict the off-design behaviour of the I-ESS during the discharge. To investigate only the discharge phase, the starting point of the TES tank is an isothermal condition.

The rest of the work is organised as follows. Section 2. describes the I-ESS layout, while Section 3. presents the off-design mathematical model of the I-ESS storage unit. Section 4. summarises the most interesting outcomes of the numerical investigation, while Section 5. states the conclusions.

## **2. Integrated Electricity Storage System (I-ESS)**

The storage plant investigated in this work is based on the configuration developed and tested by Benato et al. [7, 8]. The arrangement is named Integrated Energy Storage System; a thermomechanical unit for storing electricity in the form of sensible heat that allows the use of components of existing unused or in-decommissioning fossil power plants. In this way, the system provides flexibility to the grid without installing additional capacity.

The layout of the plant is sketched in Figure 1.

During charge, a fan guarantees the circulation of air in the storage charging circuit. Air is the heat transfer fluid. After being sucked by the fan, the air is preheated in a heat exchanger (HX) using the energy content of the air leaving the storage tank and then heated up by a resistive electric heater (EH). Hot air leaving the electric heater is at a high temperature and enters the TES tank. Air heats the solid material that constitutes the thermal energy storage tank. Therefore, electricity is stored as sensible heat because of an increase in the temperature of the storage material. The power input during the charging phase is in the fan and in the electric heater. The adoption of an EH allows the air temperature to be maintained at the input of the packed bed at a fixed value independently of the other operating conditions.

Note that in a PTES system, the storage inlet temperature is an independent variable only if the compressor's inlet conditions are constant. This is guaranteed by a heat exchanger; a component that is the source of high losses.

The discharge cycle is based on the Brayton-Joule thermodynamic cycle. In terms of components, the discharge arrangement is a gas turbine, where thermal storage replaces the combustion chamber or an air bot-

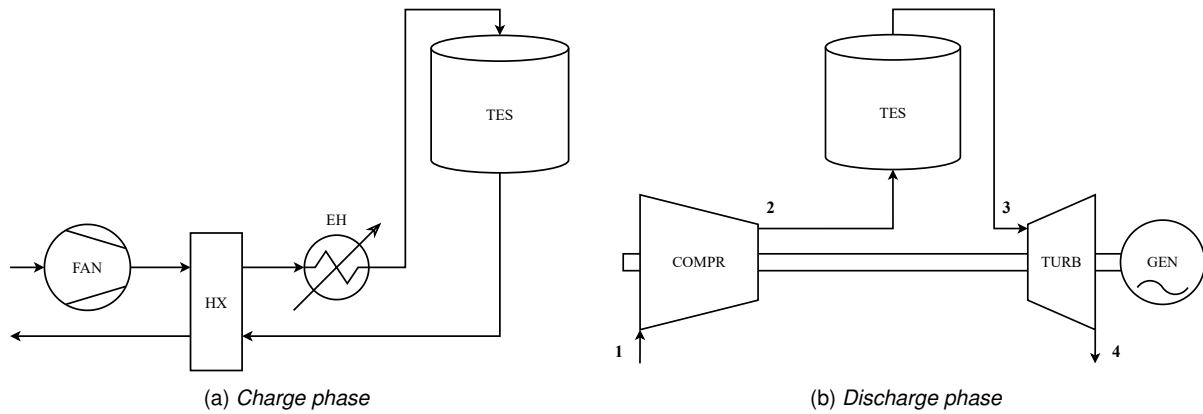


Figure 1: Layout of the I-ESS system in (a) charge and (b) discharge modes.

toring cycle in which the heat exchanger is replaced with the TES tank.

The air under ambient conditions is sucked and compressed by a compressor. Then it is heated in high-temperature TES. Consequently, the temperature of the material that makes up the TES decreases with increasing of the discharge time. Finally, the hot air expands through a turbine and returns to the atmosphere. The mechanical power generated by the turbine is converted into electricity through the electric generator. In this way, excess electricity generated by renewable sources and not requested by the grid is stored as sensible heat and then reinjected into the grid when required.

In the I-ESS configuration, the compressor and the turbine can be radial and axial turbomachines depending on the plant nameplate power. In this case, the devices are axial turbomachines that work at a constant rotational speed.

Although the layout of both working conditions is shown in Figure 1, only the discharge phase is investigated. The reason for this choice is as follows. In previous studies, it was shown that, despite poor efficiency, the investment costs of I-ESS are really competitive with other ES technologies [7]. Furthermore, a proper selection of the type and shape of solid storage material allows the plant to reduce costs, as well as design a storage facility that can store a different amount of energy in the same volume [8]. A feature that intrinsically guarantees the scalability of the plant based on the needs of the network. However, an in-depth analysis of plant behaviour under off-design conditions is still lacking. To fully understand the potential of the proposed storage system and develop custom management strategies, the decrease in turbomachine efficiency under part-load conditions must be taken into account. For these reasons, this work is focused on off-design modelling of the I-ESS system with an in-depth description of the compressor and the turbine through the use of performance maps.

### 3. The I-ESS off-design numerical model

During the delivery phase, the thermal reservoir temperature profile changes continuously. This means that the turbine inlet temperature (TIT), which is the driving parameter in calculating the equilibrium point of the system, also changes continuously. This fact leads to two important consequences. On the one hand, unlike a conventional power plant, the I-ESS never works under design conditions. Therefore, it is important to build an ad hoc mathematical model to describe its off-design behaviour. However, the system operates in a continuous transient state. Therefore, the steady-state working point does not exist.

In the already available I-ESS mathematical model, only the thermal reservoir one is dynamic, whereas the rest of the components, as well as the control strategy, are treated with a steady-state approach. This means that the model is built on the hypothesis that the time constant of the thermal phenomena is higher than the time constant of the mechanical one. With this approach, a pseudo-steady-state equilibrium point is computed at each time step.

Obviously, this way of modelling the turbomachines is widely adopted and guarantees to describe in an appropriate manner the behaviour of the system, especially if the simulation time involves the entire year. However, to predict the step response and the start-up/shut-down of the storage unit, a proper dynamic model of the whole system must be built, but this is beyond the objectives of this work because it is focused on the discharge arrangement.

The system consists of two axial turbomachines and a packed-bed thermal reservoir. The power regulation of the plant takes place by managing the angle of the variable inlet guide vanes (VIGV) at the compressor inlet, while the rotational speed of the shaft remains constant. The model is built in a Matlab environment, while the

thermophysical properties of both air and storage material are taken from the *NIST* databases.

### 3.1. The I-ESS off-design model

#### 3.1.1. The air compressor model

Turbomachines are modelled with a zero-dimensional approach. In fact, the behaviour of both the compressor and the turbine is described through their performance maps. Standard maps are taken from the database of commercial software [10] and then scaled according to the design point. The working point, which is characterised by a certain combination of pressure ratio ( $pr$ ), mass flow rate ( $\dot{m}$ ) and isentropic efficiency ( $\eta_{is}$ ), is expressed as a function of rotational speed ( $N$ ) and auxiliary coordinate  $\beta$  (see Equation 1).

$$\{pr, \dot{m}, \eta_{is}\}_c = f(\beta_c, N_c) \quad (1)$$

Due to the maps' interpolation, these values can be derived. Then, providing as input the inlet pressure and temperature, it is possible to compute the outlet conditions using Equation 2 and Equation 3.

$$p_2 = p_1 \cdot pr_c \quad (2)$$

$$T_2 = T_1 \cdot \left( 1 + \frac{1}{\eta_{is,c}} \cdot (pr_c^{\frac{\gamma-1}{\gamma}} - 1) \right) \quad (3)$$

During off-design operating conditions, the I-ESS management system varies the VIGV angle ( $\alpha_{IGV}$ ) to keep the rotational speed constant. The laws that describe the modification of the compressor working point as a function of  $\alpha_{IGV}$  are as follows.

$$a_{VIGV} = \frac{\partial \dot{m} [\%]}{\partial VIGV [^\circ]} \quad (4)$$

$$b_{VIGV} = \frac{\partial (pr_c - 1) [\%]}{\partial VIGV [^\circ]} \quad (5)$$

$$c_{VIGV} = \frac{\partial \eta_{is} [\%]}{\partial VIGV [^\circ]} \quad (6)$$

The values of the coefficients  $a$ ,  $b$ , and  $c$  are set equal to 1, 1 and 0.01 as suggested in Ref. [11]. The positive values of  $\alpha_{IGV}$  correspond to the closure of the variable inlet guide vanes. In contrast, negative values mean an opening of the VIGV compared to the design position ( $\alpha_{IGV,des} = 0$ ).

#### 3.1.2. The turbine model

The turbine is also modelled using standard maps scaled according to the design values of the pressure ratio and the corrected mass flow. As given for the compressor, the values of the mass flow rate, the pressure ratio and the isentropic efficiency are expressed as a function of the rotational speed and the auxiliary coordinate  $\beta$  (Equation 7).

$$\{pr, \dot{m}, \eta_{is}\}_t = f(\beta_t, N_t) \quad (7)$$

The turbine geometry is fixed, and there are no variable inlet guide vanes. The outlet temperature and pressure are calculated as given in Equation 8 and Equation 9.

$$p_4 = \frac{p_3}{pr_t} \quad (8)$$

$$T_4 = T_3 \cdot \left( 1 - \eta_{is,t} \left( 1 - \left( \frac{1}{pr_t} \right)^{\frac{\gamma-1}{\gamma}} \right) \right) \quad (9)$$

#### 3.1.3. The thermal energy storage with packed bed mathematical model

The thermal energy storage tank is the key component of the I-ESS plant because it allows the storage of electrical energy in the form of sensible heat.

Several models can be found in the literature for the description of the thermal reservoir [12] but, in this case, the TES-PD model developed by Benato et al. [13] is adopted. The TES-PD model is a 1D model in which

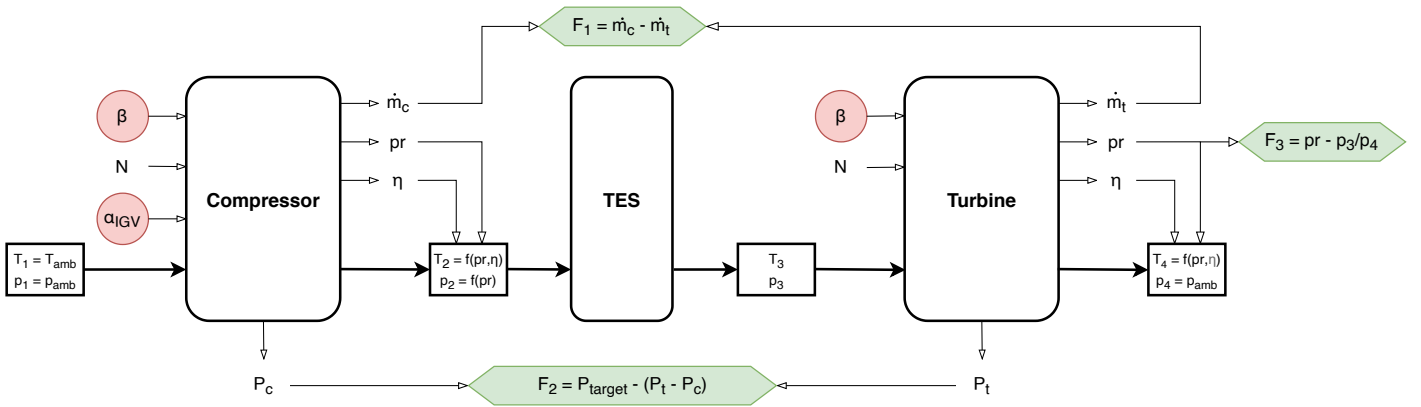


Figure 2: Scheme of the calculation for the matching procedure. The matching variables are highlighted in red, while the functions are highlighted in green.

the tank is discretised into  $n$  layers characterised by the same dimension. The influence of the number of discretisations on both the computation time and the accuracy in the calculation of the temperature profile has been thoroughly investigated in Ref. [13]. One of the peculiarities of the model is its ability to take into account the variability of the thermophysical properties of both the solid material that makes up the packed bed and the heat transfer fluid (air). For more details, the interested reader can refer to [13].

### 3.2. Components matching

The I-ESS model calculates pseudo-steady-state points, where the turbomachines are supposed to instantaneously adapt to the thermal behaviour of the reservoir. This means that for each time step, the power and the mass balance are fulfilled.

In this scenario, finding the equilibrium point of the system requires solving a system of non-linear equations of dimension three [14]. The procedure is based on the gradient-based `fsolve` algorithm available in the *Matlab* suite. It employs a variant of the Powell method (trust-region algorithm [15]). In Equation 10,  $\delta x$  is the vector that contains step changes of the matching variables,  $J$  is the Jacobian matrix, and  $F$  is the vector with errors. The matching variables are  $\beta_{compr}$ ,  $\alpha_{IGV}$  and  $\beta_{turb}$ , while the errors come from the check of the turbine pressure ratio, the mass continuity, and the power balance, as shown in Figure 2.

$$J \cdot \delta x = -F \quad (10)$$

At each iteration  $k$ , the new variables are calculated as  $x_k = x_{k-1} + \delta x$ . The system is solved when  $F = 0$ . The final values of  $\beta_{compr}$ ,  $\alpha_{IGV}$ , and  $\beta_{turb}$  are those that meet the equations of mass and power balance and give a net power equal to that set as input.

### 3.3. The I-ESS model setup

Being the aim of the work to study the off-design behaviour of the I-ESS system during the discharge process to improve the accuracy of the plant behaviour prediction, the design parameter of the system must be defined. To evaluate in future work the advantages in terms of accuracy of using compressors' and turbines' maps instead of simplified models, the I-ESS design parameters are the same as those in the work presented in Ref. [9].

In particular, the thermal storage volume is equal to 250 m<sup>3</sup>, while its height is 6.6 m. The packed bed is made up of spheres of aluminium oxide ( $Al_2O_3$ ). The density, void fraction, and diameter of the spheres are summarised in Table 1.

The design power of the power train is set at 0.8 MW, while the compressor pressure ratio and the polytropic efficiency of both turbomachines are set at 8.5 and 0.85, respectively.

Based on the design characteristics of the gas turbine used to build the I-ESS power train, the thermal reservoir design temperature, which is equal to the turbine inlet temperature, is set at 1200 K while the air mass flow during discharge is 4.42 kg · s<sup>-1</sup>.

The turbomachines have an axial arrangement. Therefore, for the compressor and the turbine, an axial map is selected from the commercial software database. Subsequently, the selected maps are scaled according to the design values. Note that this is common practise in the case of a lack of information on the performance maps of the machines considered [16].

To properly study the delivery phase, the discharge investigation is carried out starting from a TES tank under

|                   |                     |              |
|-------------------|---------------------|--------------|
| Geometry          | packed-bed          |              |
| Material          | $Al_2O_3$ (alumina) |              |
| Shape             | spheres             |              |
| TES volume        | 250                 | $m^3$        |
| TES height        | 6.6                 | $m$          |
| $Al_2O_3$ density | 3990                | $kg\ m^{-3}$ |
| Void fraction     | 0.4                 | –            |
| Spheres diameter  | 50                  | $mm$         |

Table 1: Design characteristics of the TES.

isothermal conditions (1200 K).

## 4. Results and discussion

After model validation (see, [7, 8]), a preliminary investigation is conducted with the aim of finding the technical minimum of the system. As said, for simplicity, the reservoir starts in an isothermal condition.

At the beginning of the discharge phase, the I-ESS-deliverable power is set to the nameplate one. However, in the progress of the discharge, the temperature of the packed bed decreases and, consequently, the turbine inlet temperature. Therefore, the I-ESS management system is not able to maintain both the power and the rotation speed at the design value. Then, since the control strategy is devoted to maintaining a constant rotational speed, the power delivered to the grid is reduced with the decrease in the state of charge of the TES (see Figure 3). The power reduction continues until the system can no longer provide power by maintaining a constant rotational speed. This condition corresponds to a power equal to about 40% of the design one. Taking into account the safety margin, the I-ESS technical minimum is set equal to 50% of the gas turbine nameplate power.

The analysis of the discharge phase from the full charge to the technical minimum reveals that, as the TIT changes, the equilibrium point of the system also changes. Therefore, to maintain the rotational speed constant, the angle of the VIGVs must be continuously adjusted (Figure 3). The initial value of  $\alpha_{IGV}$ , when the VIGVs are in the design condition, is  $\alpha_{IGV} = 0$ . Initially, to maintain the rated power, the VIGVs have to slightly open to counterbalance the decrease in the TIT. Then, when the power is scaled,  $\alpha_{IGV}$  suddenly increases to a positive value (Figure 4).

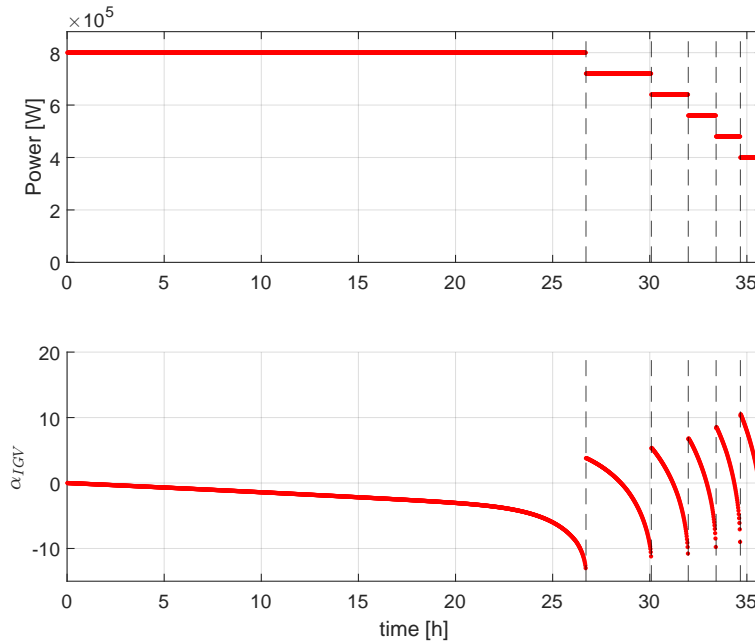


Figure 3: Power trend and  $\alpha_{IGV}$  trend over time.

As said, during the delivery phase, the temperature of the packed bed decreases. Figure 5 shows the temperature trend of some layers over time. It is interesting to note that the temperature of the first layers quickly drops to 600 K, which is the compressor outlet temperature. The first layer is slightly heated after some time

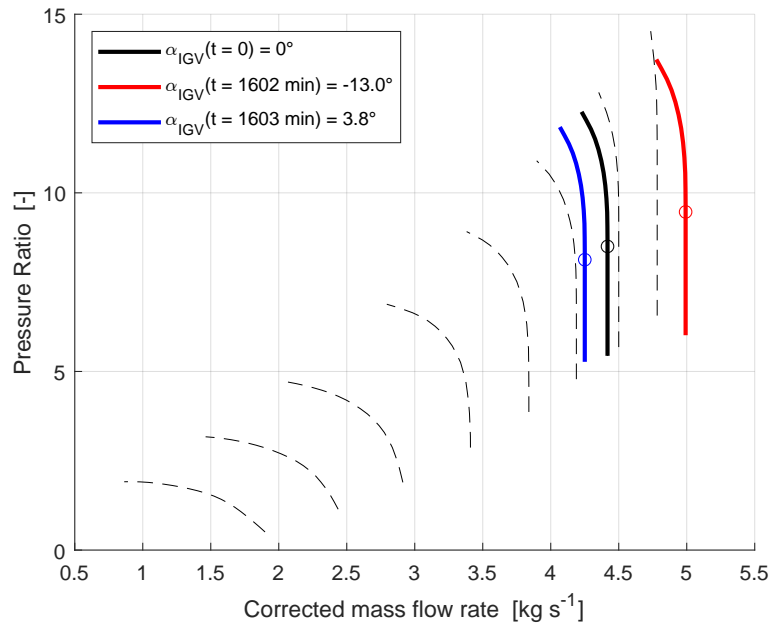


Figure 4: Shift of the speedline according to  $\alpha_{IGV}$ .

step, and this is due to an increase in the compressor pressure ratio related to the regulation of  $\alpha_{IGV}$ .

The discontinuities in the temperature trend come from the step regulation of the net power, as shown in Figure 3. The graph in Figure 5 also shows the trend of TIT over time. The TIT follows the trend of the last layers of the reservoir.

Figure 6 shows the thermodynamic cycle at both the beginning and the end of the discharge. Note that, at the end of discharge, both  $\eta_{is,c}$  and  $TIT$  are lower compared to the design point.

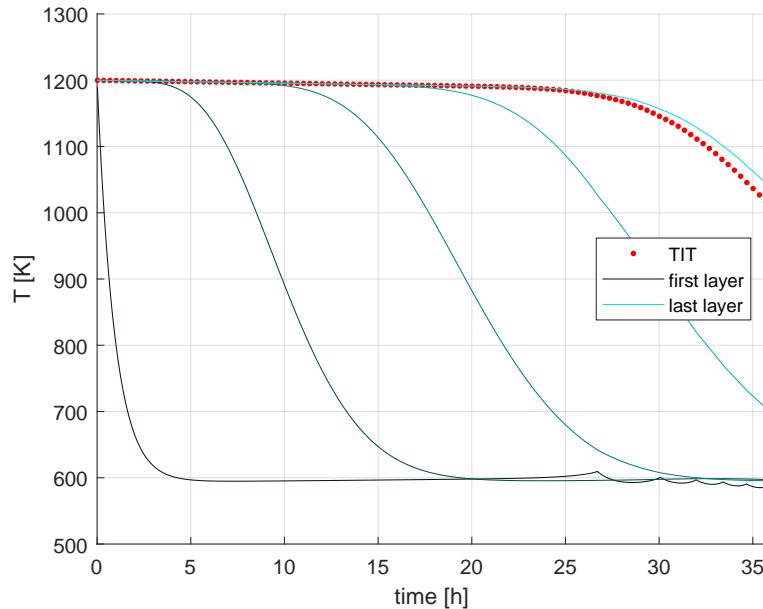


Figure 5: Temperature trend of some sample layers and TIT trend over time.

The choice of the number of layers for the discretisation of the packed bed influences the accuracy of describing the thermofluid dynamics of the reservoir [13]. However, the focus of this work is to study the performance of the whole system, rather than the thermal storage itself. Therefore, a sensitivity analysis is performed to evaluate the effect of the number of layers ( $n$ ) on the accuracy of the model.

The turbine inlet temperature is selected as a key parameter as the driving variable in the calculation of the thermodynamic cycle. The analysis revealed that, varying  $n$  from 30 to 160 with a step of 30, the standard deviation in the TIT calculation at the end of discharge is approximately 0.02%. For this reason, a number of 60 layers is chosen as a good compromise between computational speed and accuracy.

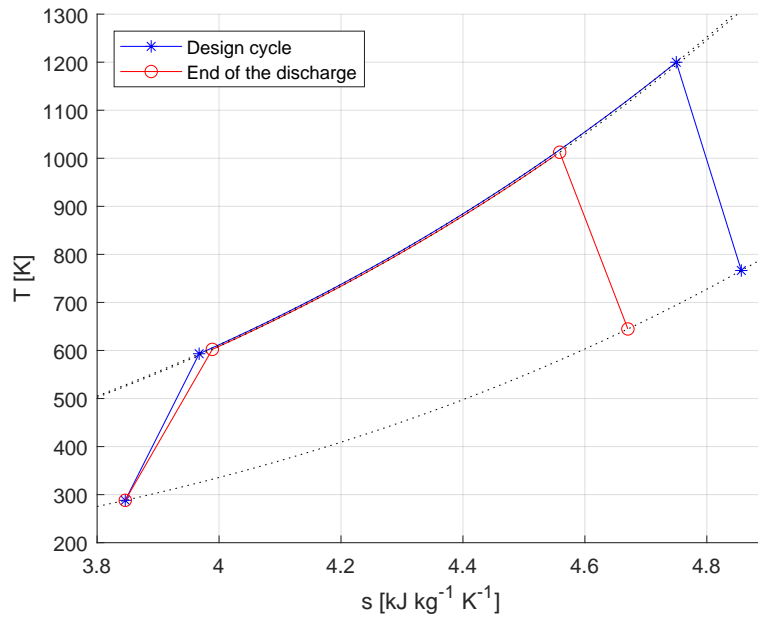


Figure 6: Thermodynamic cycle at the design point and at the end of the discharge.

After this preliminary investigation devoted to the definition of the technical minimum and the number of layers in which storage needs to be discretised, it is interesting to study the total discharge time and the discharge time at nameplate power by varying by the tank temperature, the design power and the power step size.

Figure 7 shows the influence of design parameters on the total discharge time and the discharge duration at the nameplate power.

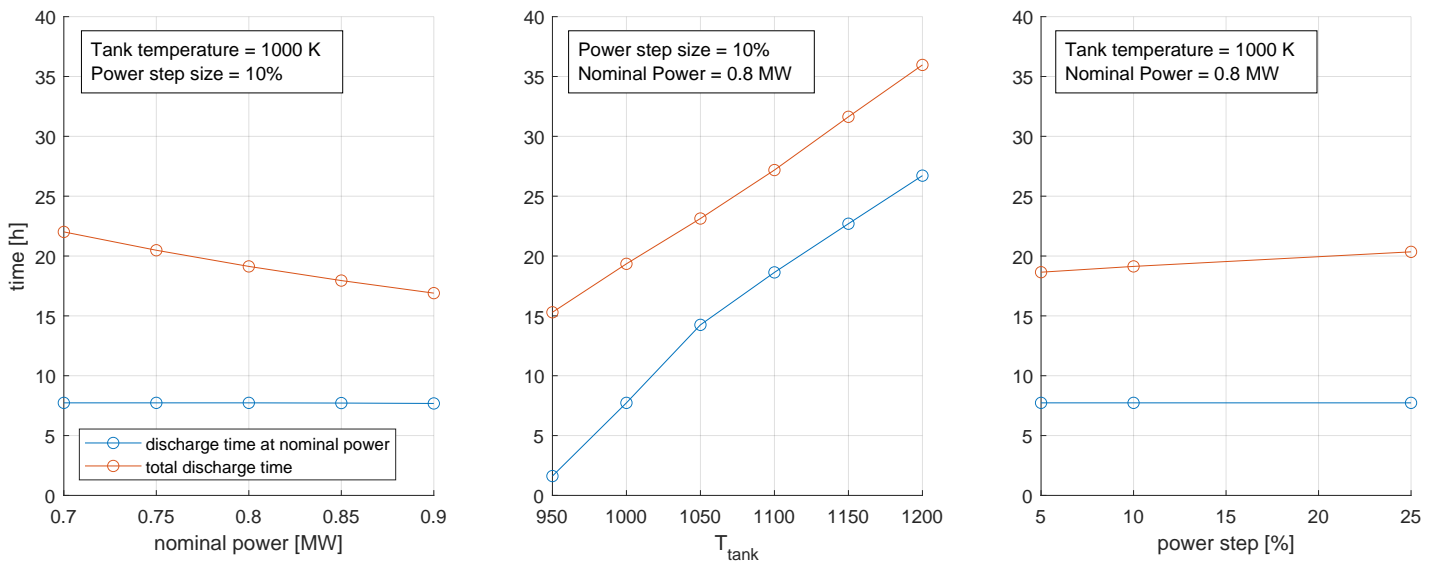


Figure 7: Influence of design parameters on the total discharge time and the discharge duration at nameplate power.

The discharge time at nameplate power is strongly influenced by the reservoir temperature: the higher the temperature, the longer the time for which the system can deliver the nameplate power.

The nameplate power and the power step size do not affect discharge duration. Furthermore, the total discharge time increases rapidly if the storage temperature increases, while it increases only slightly with the power step size. However, the total discharge time decreases if the nominal power is high.

It is also interesting to analyse the maximum thermal energy that can be stored in the tank. With the hypothesis of heating the tank from ambient temperature (293 K) to 1200 K, the maximum storable thermal energy is  $201.6 \text{ MWh}_{th}$ .

Taking into account the full discharge, the maximum exploitable energy can be calculated as:



$$E_{th,discharge} = M \cdot \frac{1}{n} \cdot \sum_{j=1:n} \left( \int c_p(T) \cdot dT \right) \quad (11)$$

where  $n$  is the number of layers,  $M$  is the mass of the solid and  $c_p$  is the specific heat of the solid.

Given the technical minimum fixed at 50%, the maximum exploitable thermal energy is 106.1  $MWh_{th}$ , which results in 26.9  $MWh_{el}$ .

Note that, for the hypothesis of the investigation performed, the charge phase is not modelled. Therefore, the Round-Trip Efficiency (RTE) cannot be defined on the basis of the selected starting state of charge.

However, considering the TES isothermal (not reachable condition) at a temperature of 1200 K, the efficiency of the discharge phase can be computed as

$$\eta_{discharge} = \frac{E_{el,discharge}}{E_{th,discharge}} \quad (12)$$

and resulted equal to 25.3%.

## 5. Conclusions

The off-design performance of an Integrated Electricity Storage System (I-ESS) has been analysed in this study. To this end, a proper off-design model of the plant has been built. The model takes into account the part-load behaviour of the turbomachines with a zero-dimensional approach using performance maps. Although it includes a dynamic description of the Thermal Energy Storage, the model of the system calculates pseudo-steady-state points. In this way, the behaviour of the plant during a complete discharge can be studied, starting from an isothermal reservoir. The results show that the temperature of the reservoir is the parameter that affects primarily the performance of the plant in the delivery mode.

With an increase in tank temperature, both the total discharge time and the nameplate power discharge time increase. In contrast, as the design power is increased, the total duration of the discharge decreases. In addition, the power step size has a smaller influence on these parameters.

The results also show that the number of layers for TES discretisation is not as relevant for the calculation of the performance of the whole system. Therefore, this parameter can be kept to the minimum possible to speed up the computation time without significantly affecting the model accuracy. The efficiency of the delivery phase, for the selected working conditions, is equal to 25.3%. Future developments will involve the implementation of off-design characteristics of the fan, electric heater, and heat exchanger in the charging model. In this way, the round-trip efficiency can be defined and computed as well as the thermodynamic and economic performance of the full operation of the system. After that, the dynamic behaviour can be analysed and tailor-made management strategies developed based on grid needs.

## Nomenclature

### Abbreviations

|              |                                       |
|--------------|---------------------------------------|
| <i>CAES</i>  | Compressed Air Energy Storage         |
| <i>CB</i>    | Carnot Battery                        |
| <i>EH</i>    | Electric Heater                       |
| <i>ES</i>    | Energy Storage                        |
| <i>FB</i>    | Flow Batteries                        |
| <i>HX</i>    | Heat Exchanger                        |
| <i>I-ESS</i> | Integrated Electricity Storage System |
| <i>LAES</i>  | Liquid Air Energy Storage             |
| <i>PHS</i>   | Pumped Hydro Storage                  |
| <i>PTES</i>  | Pumped Thermal Energy Storage         |
| <i>RES</i>   | Renewable Energy Storage              |

TES Thermal Energy Storage

TIT Turbine Inlet Temperature

VIGVs Variable Inlet Guide Vanes

### Constants and variables

$c_p$  specific heat, J/(kgK)

$\dot{m}$  mass flow rate, kg s<sup>-1</sup>

$N$  rotational speed

$n$  number of layers

$pr$  pressure ratio

$T$  temperature

$\alpha_{IGV}$  Variable Inlet Guide Vanes position

$\beta$  auxiliary coordinate of turbomachinery performance maps

$\eta_{is}$  isentropic efficiency

### Subscripts and superscripts

$c$  compressor

$t$  turbine

$el$  electrical

$th$  thermal

### References

- [1] Andrea Vecchi et al. "Carnot Battery development: A review on system performance, applications and commercial state-of-the-art". In: *Journal of Energy Storage* 55 (Nov. 2022), p. 105782. ISSN: 2352152X. DOI: 10.1016/j.est.2022.105782.
- [2] Alessandro Lampasi et al. "Review of Carnot Battery Technology Commercial Development". In: (2022). DOI: 10.3390/en15020647.
- [3] Olivier Dumont et al. "Carnot battery technology: A state-of-the-art review". In: *Journal of Energy Storage* 32 (2020), p. 101756.
- [4] Tristan Desrues et al. "A thermal energy storage process for large scale electric applications". In: *Applied Thermal Engineering* 30.5 (2010), pp. 425–432.
- [5] Joshua D McTigue, Alexander J White, and Christos N Markides. "Parametric studies and optimisation of pumped thermal electricity storage". In: *Applied Energy* 137 (2015), pp. 800–811.
- [6] Alberto Benato. "Performance and cost evaluation of an innovative Pumped Thermal Electricity Storage power system". In: *Energy* 138 (2017), pp. 419–436.
- [7] Alberto Benato and Anna Stoppato. "Energy and cost analysis of an Air Cycle used as prime mover of a Thermal Electricity Storage". In: *Journal of Energy Storage* 17 (2018), pp. 29–46.
- [8] Alberto Benato and Anna Stoppato. "Integrated thermal electricity storage system: Energetic and cost performance". In: *Energy Conversion and Management* 197 (2019), p. 111833.
- [9] Alberto Benato, Francesco De Vanna, and Anna Stoppato. "Levelling the Photovoltaic Power Profile with the Integrated Energy Storage System". In: *Energies* 15.24 (2022), p. 9521.
- [10] J Kurzke. *Gasturb 12: A program to calculate design and off-design performance of gas turbines. users manual*. 2012.
- [11] Muhammad Baqir Hashmi, Tamiru Alemu Lemma, and Zainal Ambri Abdul Karim. "Investigation of the Combined Effect of Variable Inlet Guide Vane Drift, Fouling, and Inlet Air Cooling on Gas Turbine Performance". In: *Entropy* 21.12 (2019). ISSN: 1099-4300. DOI: 10.3390/e21121186.

- [12] Alexej Paul et al. "High temperature sensible thermal energy storage as a crucial element of Carnot Batteries: Overall classification and technical review based on parameters and key figures". In: *Journal of Energy Storage* 56 (Dec. 2022). ISSN: 2352152X. DOI: 10.1016/j.est.2022.106015.
- [13] Alberto Benato et al. "TES-PD: A Fast and Reliable Numerical Model to Predict the Performance of Thermal Reservoir for Electricity Energy Storage Units". In: *Fluids* 6.7 (2021), p. 256.
- [14] AMY Razak. *Industrial gas turbines: performance and operability*. Elsevier, 2007.
- [15] Michael JD Powell. *A Fortran subroutine for solving systems of nonlinear algebraic equations*. Tech. rep. Atomic Energy Research Establishment, Harwell, England (United Kingdom), 1968.
- [16] Andrea Lazzaretto and Toffolo Andrea. "Analytical and Neural Network Models for Gas Turbine Design and Off-Design Simulation". In: *International Journal of Thermodynamics* 4 (Dec. 2001). DOI: 10.5541/ijot.78.